Global NEST Journal, Vol 23, No 1, pp 104-110

Modified Mangosteen shell carbon in the removal of Pb (II) and Hg (II) from aqueous solution – isotherm and kinetic studies

Anitha D.[1*] and Ramadevi A.[2]
[1]Department of Chemistry, Karpagam Institute of Technology, Coimbatore, India, 641105
[2]Department of Chemistry, Government College of Technology, Coimbatore, India, 641013
Received: 19/07/2019, Accepted: 19/12/2020, Available online: 15/01/2021
*to whom all correspondence should be addressed: e-mail: devasahayamanitha@gmail.com
https://doi.org/10.30955/gnj.003188

Graphical abstract

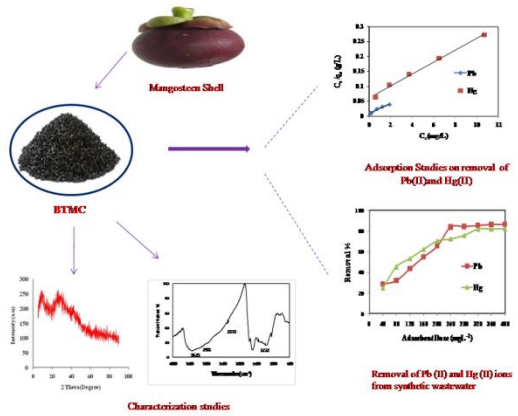

Abstract

An adsorbent was prepared from Mangosteen shell using sulphuric acid and sodium bicarbonate as modifiers. Bicarbonate treated mangosteen shell (BTMC) was characterized using FT-IR, SEM, EDAX and XRD data. The Freundlich adsorption isotherm model gives a good fit. The maximum adsorption capacities of BTMC were found to be 58.48 mg g-1 and 49.75 mg g-1 for Pb (II) and. Hg (II). Adsorption of Pb (II) and Hg (II) followed pseudo-second-order kinetics. The adsorption mechanism was explained using the Weber and Morris's intra-particular diffusion process. Batch mode studies with synthetic wastewater suggest that BTMC can be efficiently used in wastewater treatment.

1. Introduction

Heavy metals act as prime pollutants in the sea, ground, industrial and even treated wastewaters. Heavy metal pollution in water is of serious concern as they bioaccumulate in the food chain and cause unfavourable consequences to the environment. To a minor range, they pass into human bodies through food, drinking water and air. Major sources of Lead are lead-acid batteries, paints, E-waste, Smelting operations, coal-based thermal power plants, ceramics, bangle industry and Mercury are Chloro-alkali plants, thermal power plants, fluorescent lamps and electrical appliances (Verma and Dwivedi, 2013). Lead is one among the poisonous heavy metal which is hazardous to human health even at low concentration (Bahrami *et al.,* 2014). It affects the nervous system causing blood and brain disorders (Ebrahimzadeh *et al.,* 2015).

Mercury is also priority pollutants which can easily diffuse through the blood-brain barrier and affect the fetal brain. High concentration of Hg (II) causes impairment of pulmonary function and kidney, chest pain and dyspnea (Zabihi *et al.,* 2009).

Low-cost adsorbents derived from agricultural by-products and industrial solid wastes could be used to remove recalcitrant wastes from synthetic wastewater (Lakherwal, 2014). At recent times great significance is emphasized on the manufacture and understanding of the sorption properties of alternative low-cost materials (Akunwa *et al*., 2014). The adsorption capacities of such adsorbents are not great as expected and the search for new adsorbents is still under progress (Senthil Kumar *et al*.,2013). Agricultural waste peel like wheat barn (Ozer, 2007) Lansium domesticum peel (Lam *et al*., 2016) Palm shell (Ismail *et al*., 2013) chestnut shell (Yao *et al*., 2010) Pistachio shell carbon (Shaziya *et al.,* 2016) grapefruit peel (Mostaedi *et al*., 2013) are used in the removal of heavy metals from water.

Mangosteen (Garcinia Mangostana Linn.) belongs to the Hypericaceae family which is available in plenty in Asian countries. The pericarp (outer shell or rind) is hard and when 10 kg of mangosteen harvested, an average of 6 kg of mangosteen peel is generated (Chen *et al*., 2011).The phenolic acid present in the pericarp of mangosteen shell has good ability to bind heavy metals from the aqueous solution (Zadernowski *et al*., 2009). In the present study, mangosteen shell was modified using sulphuric acid and sodium bicarbonate solution and its removal efficiency were examined using an aqueous solution of lead and mercury.

2. Materials and methods

2.1. Preparation of adsorbent

Mangosteen shell was washed with distilled water, dried to 110 °C powdered and sieved using 20-50 ASTM mesh. It

was treated with a con H_2SO_4 (1:1) weight ratio and kept in a hot air oven at 150±5 °C for 24 h. The carbonized material obtained was washed with distilled water to remove the free acid and soaked in 1% sodium bicarbonate until the effervescence ceases and further soaked in the same solution for 24 h to remove the residual acid. The adsorbent obtained was again washed with distilled water, dried and sieved to 20-50 ASTM mesh size and labeled as Bicarbonate Treated Mangosteen Shell carbon (BTMC).

2.2. Batch adsorption experiments

Adsorption studies were carried out by varying contact time (30-210 min), solution pH (1-10) and adsorbent dosage (40-280 mg). For each study a required quantity of adsorbent dose was added to 100 mL of 10 mg L^{-1} of metal ion solutions taken in a polythene container agitated in a mechanical shaker. The carbon was separated by filtration and the filtrate was analyzed for Pb (II) and Hg (II) by spectrophotometer using PAR [4-(2-pyrodylazo) resorcinol] reagent for Pb (II) content. (Pollard, 1957) Rhodamine 6G reagent (Mc Kay *et al.,* 1982) for Hg (II) using standard experimental procedure.

3. Results and discussion

3.1. FT-IR, SEM, EDAX and XRD analysis

Fourier transform infrared spectroscopy (FT-IR) studies were used to identify the functional groups present on the surface of the adsorbent. The FT-IR spectrum of BTMC Figure 1a shows the presence of polyfunctional groups. The strong absorption peak at 3425 cm^{-1}, is due to the -OH stretching vibration due to inter and intramolecular hydrogen bonding of alcohols, phenols, and carboxylic acids. The peaks at 2981 cm^{-1}, 2372 $cm,^{-1}$ and 1222 cm^{-1} are due to the C-H stretching, C⩝C stretching and -CO stretching vibration of ether. The presence of a sulphonic acid group is confirmed by the peak at 1446 cm^{-1}. From the IR spectrum of Pb (II) and Hg (II) adsorbed carbon, Figure 1(b and c) it is evident that some of the peaks shift or become weak indicating the incorporation of heavy metal ion Pb (II) and Hg (II) within the adsorbent through the interaction of the active functional group after adsorption.

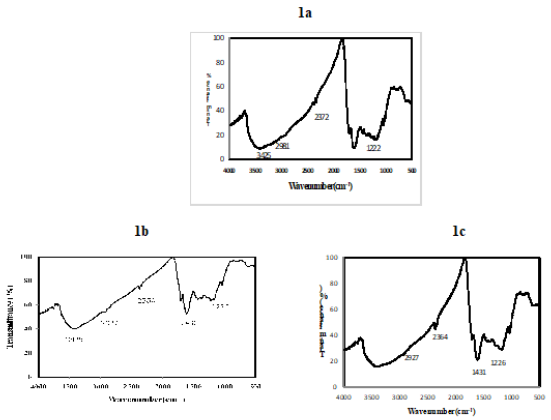

Figure 1. (a–c) FTIR spectra of BTMC , Pb(II) and Hg (II) adsorbed spectra

The surface morphology of adsorbent was found based on a scanning electron microscope. The modification in the surface morphology due to metal adsorption can be easily identified by comparing SEM micrographs of adsorbent and metal bonded adsorbent. This microscope image in Figure 2a shows the presence of isolated pores of varying dimensions before and after adsorption. The cave-like opening before adsorption of heavy metal is clearly seen in BTMC (Figure 2a) and filled with Pb(II) and Hg (II) ion after adsorption.(Figure 2b and c).

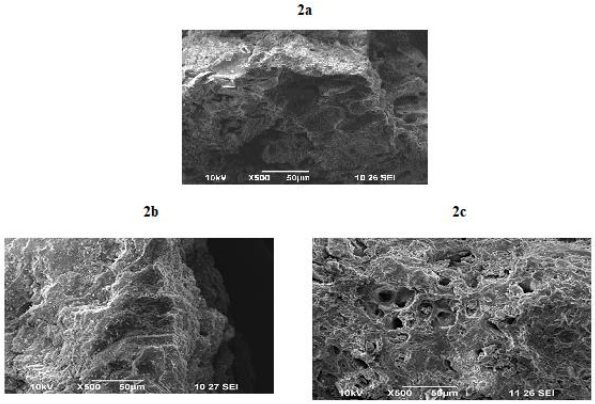

Figure 2. (a–c) SEM of BTMC, after adsorption of Pb(II), after adsorption of Hg(II)

Energy-dispersive X-ray analysis helps to confirm the elements present in the adsorbent before and after adsorption of the metal ions. Energy-dispersive X-ray analysis (EDAX) spectrum of BTMC (Figure 3a) represented peaks of C, O and Na, In the spectrum of metal-laden BTMC it was observed that signals of Na were replaced by signal of Pb, Hg which suggested that ion-exchange mechanism was involved in adsorption of lead and mercury on BTMC (Figure 3b and c).

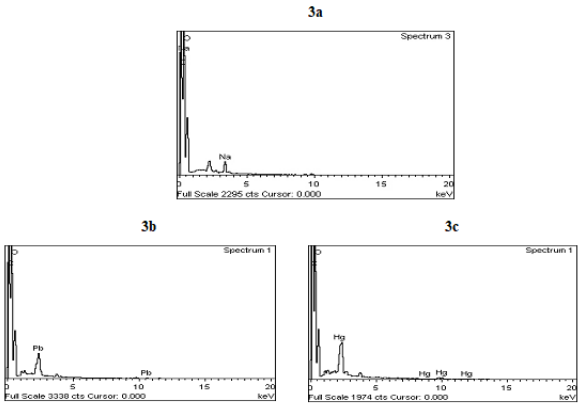

Figure 3. (a–c) EDX of BTMC, after adsorption of Pb(II), after adsorption of Hg(II)

The X-ray Diffraction (XRD) pattern of BTMC (Figure 4a) shows amorphous nature due to the presence of cellulosic material. (Shifting of peak was noted in Pb (II), Hg (II) adsorbed BTMC due to the binding of lead and mercury on BTMC (Figure 4b and c).

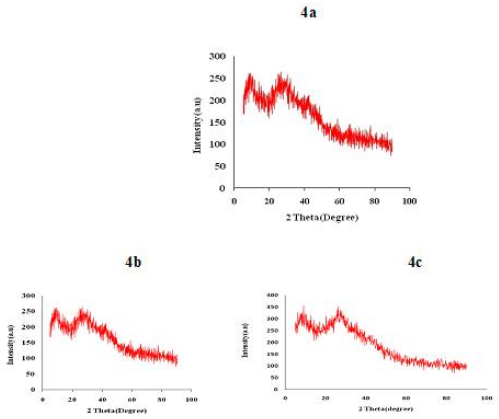

Figure 4. (a–c) XRD of BTMC, after adsorption of Pb (II), after adsorption of Hg (II)

3.2. Effect of contact time

Contact time is an important parameter to know about the adsorption process. Figure 5 shows the effect of contact time on the adsorption of Pb (II) and Hg (II) on BTMC. The contact time for the removal of Pb (II) was 30 min and Hg(II) was 120 min using BTMC. Initially ,the adsorption is faster as all adsorption sites are vacant. When the contact time increases the sites are occupied by the adsorbent resulting in a decrease in the adsorption rate. When equilibrium is reached, the adsorption slows down and the concentration of metal ion remaining in the solution is used to determine the adsorbent capacity (Banerjee *et al.,* 2012).

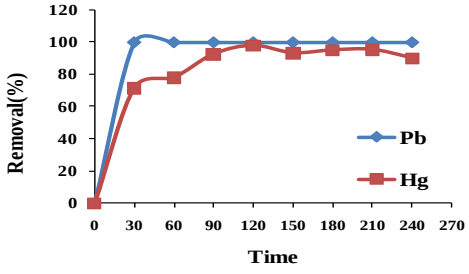

Figure 5. Effect of contact time on the removal of Pb(II) and Hg(II) by BTMC

3.3. Effect of pH

The pH of a solution is an important parameter that affects the biosorption process as the protons may alter the surface charge of bio sorbent, and the degree of ionization and speciation of metal ion (Sudha *et al*., 2015). Figure 6.

3.4. Effect of carbon dosage

The adsorbent dose is an important parameter in the biosorption of metal ions from aqueous solution owing to its effect on the number of metal ions removed per unit mass of the adsorbent (Miretzky *et al*., 2008).

It was observed from the Figure 7 that an increase in carbon dosage increases the percentage removal of Pb (II) and Hg (II) from aqueous solution as the number of available sites is more. But after attaining equilibrium i.e. 40 mg and 120 mg for Pb (II) and Hg (II) further increase in mass did not show any increase in adsorption. At this position, almost all the metal ions might have been removed so that a further increase in the carbon dosage will not bring about appreciable change in adsorption (Oyedeji *et al.,* 2010).

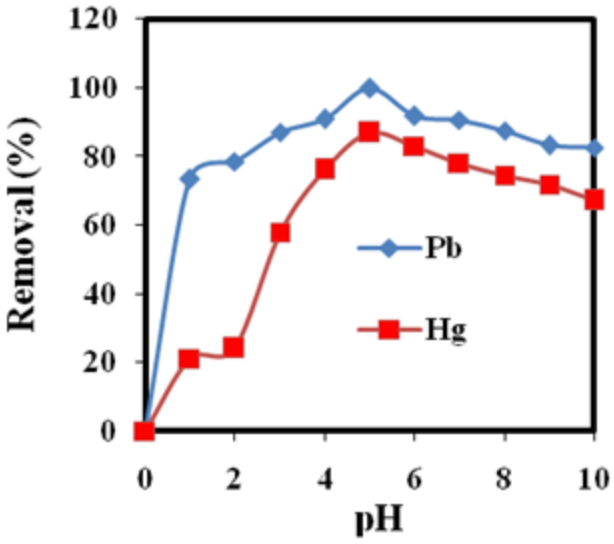

Figure 6. Effect of pH on the removal of Pb(II),Hg(II)and Ni (II) by BTMC

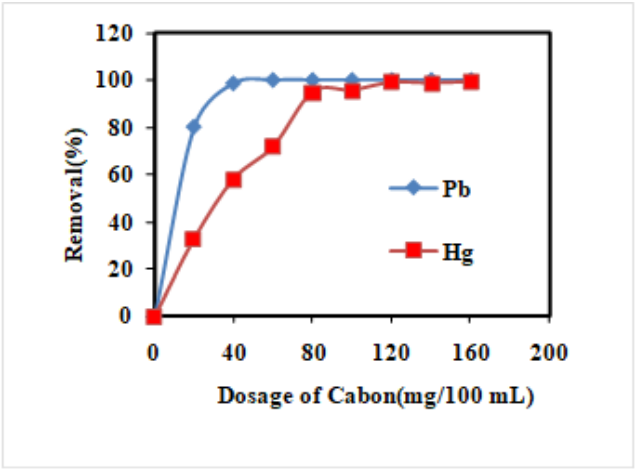

Figure 7. Effect of carbon dosage on the removal of Pb (II) and Hg (II) by BTMC

3.5. Isotherms study

Adsorption isotherms are essential in the design of batch adsorption systems (Ferreira *et al.*, 2015; Foo and Hameed, 2010). Langmuir, Freundlich, and Temkin isotherm were used to study the adsorption process and constant parameters were calculated.

The Freundlich, equation is given by

$$\log \frac{x}{m} = \log K + \frac{1}{n}(\log C\, e) \qquad (1)$$

where C_e is the equilibrium concentration (mg L^{-1}) and x/m is the amount adsorbed per unit weight of adsorbent (mg g^{-1}) and Freundlich constants *K*, *n* can be obtained from the graph between log(x/m) versus log C_e.

The empirical equation for Langmuir is given by

$$\frac{Ce}{qe}=\frac{1}{Qo}b+\frac{Ce}{Qo} \quad (2)$$

Where C_e is the equilibrium concentration (mg g^{-1}), q_e is the amount adsorbed at equilibrium (mg g^{-1}) and Q_o and b are Langmuir constants related to adsorption capacity and energy of adsorption respectively.

Temkin equation is given by

$$q_e = A + B\ ln\ C_e \quad (3)$$

where q_e is the amount of solute adsorbed by the equilibrium concentration of a metal ion in mg g^{-1} .C_e is the equilibrium of the solute in mg g^{-1}. A is the Temkin constant related to adsorption capacity in mg g^{-1} and B is the Temkin constant related to the intensity of adsorption in L mg^{-1}.

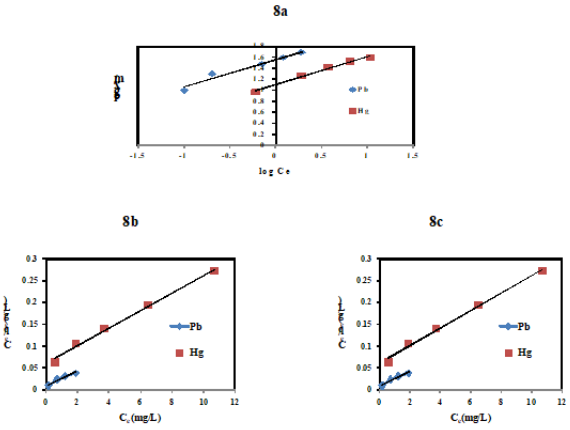

Figure 8. (a–c) Freundlich, Langmuir, Temkin adsorption isotherm for Pb(II) & Hg(II)

Langmuir, Freundlich and Temkin plots were shown in Figure 8(a–c).

Table 1. Isotherm parameters for the removal of Pb (II) and Hg (II) from aqueous solution

Isotherm model	Parameter	Pb	Hg
Freundlich	K(mg g^{-1})	200.49	127.19
	n (L^{-1} mg)	1.68	1.98
	R^2	0.919	0.991
Langmuir	Q_0(mg g^{-1})	58.48	49.75
	b (L^{-1} mg)	1.92	0.3284
	R^2	0.969	0.994
	R_L	0.215-0.838	0.06-0.23
Temkin	A	12.04	10.54
	B	37.06	13.35
	R^2	0.9720	0.9860

As indicated from Table 1 the coefficients of determination (R^2) of models were more or less greater than 0.9 indicating that these models were adequately describing the experimental data of metal biosorption experiments. Similar results were obtained (Hussein *et al.,* 2004), on their studies of heavy metals bio sorption from wastewater using Pseudomonas sp and (Mohamed *et al.,* 2012) on orange peel.

The R_L values indicates whether the type of isotherm is linear (R_L=1), favourable (0<R_L<1), unfavourable (R_L>1). (Gupta and Gogate, 2015).

In the present study, the R_L values were found to be<1, indicating the favorable biosorption of Lead and mercury on BTMC .Similar observation was noted for adsorption of lead on Cucumber peel (Basu *et al.,* 2017).

The Q_0 value of Pb (II) and Hg (II) were found to be 58.48 and 49.75 which is acceptable compared with the values observed in the literature (Rao *et al.,* 2008)

3.6. Adsorption kinetics

To investigate the adsorption of heavy metal on the surface of BTMC, different kinetic models are used to examine the controlling mechanism of the adsorption process. In the present study, the pseudo-first-order kinetic model and pseudo-second-order kinetic model were studied to find the best-fitted model for the experimental data.

The pseudo-first-order rate kinetic equation of Lagergren is expressed as: (Ahmad *et al.,* 2012).

$$\log(qe - qt) = \log q\ e - k1\frac{t}{2.303} \quad (4)$$

where q_e (mg g^{-1}) and q_t (mg g^{-1}) are the amounts of adsorption at equilibrium and at time t (min) respectively. k_1 (g mg^{-1} min^{-1}) is the rate constant of the pseudo-first order reaction.

The values of k_1 and q_e were evaluated from the linear plots of log (q_e–q_t) versus t for different concentrations of metal ions. The comparison of the experimental results and calculated values of the contact time for different concentrations of metal ions is shown in Figure 9(a and b). The calculated q_e values disagree with the experimental q_e values. Similar observations were noted by (Senthil Kumar *et al.,* 2011).

The pseudo-second-order equation based on equilibrium adsorption is expressed as:

$$\frac{t}{q_t}=\frac{1}{K_2}q_e 2 + \frac{t}{q_e} \quad (5)$$

where q_e is the amount of metal ion adsorbed in equilibrium in mg g^{-1}, q_t is the amount of metal ion adsorbed at time t, k_2 (g mg^{-1} min^{-1}) is the rate constant for the adsorption process (Sharma and Bhattacharyya, 2004). The k_2, q_e and regression coefficient value (R^2) under different concentrations were calculated from the linear plot of t/q_t vs t as shown in Figure10(a and b).

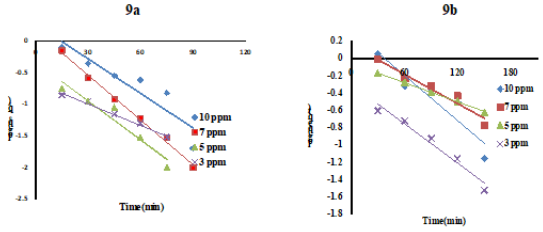

Figure 9. (a and b) Pseudo First order kinetics of Pb (II) and Hg (II) on BTMC

The pseudo-second-order model (R_2>0.99) represents the sorption kinetics better, indicating that the sorption process is controlled by chemisorption process. Similar observation was noted by (Liu *et al*., 2015).

The calculated q_e values for pseudo second-order equation are in good agreement with the experimental values .Therefore the sorption reaction belongs to the pseudo-second-order kinetic model and that the overall rate of the metal adsorption process appears to be controlled by the chemical process via ion exchange and/or complexation process (Coelho *et al.,* 2014; Jin *et al.,* 2012).

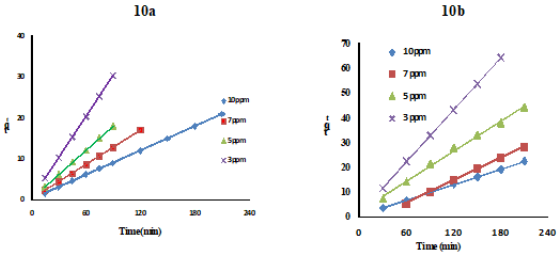

Figure 10. (a and b) Pseudo Second order kinetics of Pb (II) and Hg (II) on BTMC

Cruz *et al.*, (2004) who compared a pseudo-first-order Lagergren model and a second-order model, similarly found that the second-order model was superior for the binding of divalent cations by the brown alga Sargassum. They concluded that the biosorption reaction was the rate-limiting step.

3.7. Adsorption mechanism

The steps involved in adsorption process are explained by the following steps (Ayranci and Duman, 2005).

The movement of adsorbate molecules from the bulk to external surface of the adsorbent (Film diffusion).

The adsorbate move to the interior surface of the adsorbent particle (Intraparticle diffusion).

Adsorption of the solute on the interior surface of the pores and capillary spaces of the adsorbent (Adsorption).

Table 2. Pseudo-first-order and pseudo-second-order and Intra Particular diffusion coefficient for Pb(II), Hg(II) on BTMC at different initial concentration.

		Pseudo First Order					Pseudo Second Order				
Metal	**Con (mL^1)**	**$q_{e\,(exp)}$ (mg^1g)**	**$q_{e\,(cal)}$ (mg^1g)**	**K_1 (gmg^{-1} min^{-1})**	**P%**	**R^2**	**$q_{e(cal)}$ (mg^1g)**	**K_2 (gmg^{-1} min^{-1})**	**P%**	**R^2**	**K_{id}**
Pb	10	9.96	1.78	0.018	82.13	0.842	10.10	0.617	1.42	1	0.071
	7	6.98	1.46	0.023	79.08	0.994	7.11	0.140	1.82	1	0.092
	5	4.98	2.14	0.025	57.03	0.928	5.03	0.215	0.96	1	0.033
	3	2.99	1.29	0.112	56.86	0.988	2.99	0.459	0.07	1	0.002
Hg	10	9.35	2.13	0.0087	77.21	0.875	9.61	0.018	2.67	1.000	0.119
	7	6.50	1.45	0.0057	77.69	0.942	6.62	0.007	1.85	0.999	0.105
	5	4.75	1.14	0.0037	76	0.999	4.93	0.020	3.62	0.998	0.086
	3	2.80	2.00	0.0076	28.57	0.961	2.87	0.067	2.28	1.000	0.023

3.8. Weber-Morris intra-particle diffusion model

The kinetic data fit well to chemisorption model, to verify the influence of mass transfer resistance on the binding of Pb (II) and Hg (II) to the adsorbent and to confirm diffusion mechanism Weber and Morris intra-particle diffusion model was given by

$$q_t = K_{id} t^{1/2} \quad (6)$$

Where q_t is the amount adsorbed per unit mass of adsorbent (mg g^{-1}) at time t (min) and K_{id} is the intra-particle diffusion rate constant (mg g^{-1} $min^{-1/2}$). If the intra-particle diffusion is involved in the adsorption process, then a plot of the amount of metal ion adsorbed per unit mass of adsorbent (q_t) against square root of time ($t^{1/2}$) will give a straight line and the particle diffusion would be the controlling step if this line pass through the origin (Figure 11 a and b). However, in both Pb (II) and Hg (II) the plots were not linear and do not pass through the origin. The plot shows that intra particle-diffusion was not the only rate limiting step but also rate controlling step for adsorption or both process may operate simultaneously.

3.9. Boyd's kinetic model

The Boyd kinetic plot helps to determine the rate determining step involved in adsorption process. The Boyd's kinetic equation (Boyd *et al.,* 1947) is given by

$$F=1-6/\pi^2 \exp(B_t) \quad (7)$$

Where $F=q_e/q_t$ F represents the amount of heavy metal adsorbed at time t. B_t is the mathematical function of F.Eq (7) can be rearranged to

$$B_t=-0.4977 - \ln(1-F) \quad (8)$$

The plot of B_t versus t can be used to test the linearity of experimental values. If the plots are linear and pass through the origin the slowest step in the adsorption process is internal diffusion. From Figure 12a and b it was noted that the plots are linear but do not pass through the origin inferring that the adsorption process is controlled by film diffusion.

Figure 11. (a and b) Intra-particular diffusion plot for the adsorption of Pb (II) Hg (II) ion on BTMC

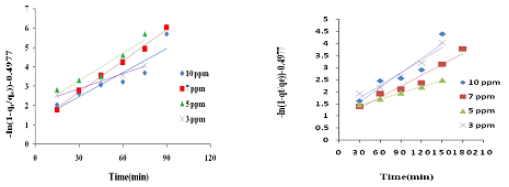

Figure 12. (a and b) Boyd's kinetic plot for the adsorption of Pb (II) Hg (II) ion on BTMC

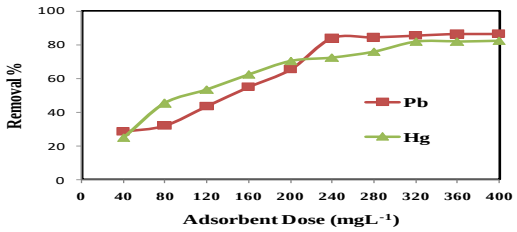

Figure 13. Removal of Pb (II) and Hg (II) ions from synthetic wastewater (Con: 10 mg L^{-1}, pH: 5 and contact time: 3 h for BTMC).

3.10. Removal of Pb (II) and Hg (II) from synthetic wastewater

The applicability of sorbent was tested by performing batch mode studies. The effect of adsorbent dosage on the removal of Pb (II) and Hg (II) from synthetic wastewater was analysed. Figure 13 shows the effect of adsorbent dosage on the removal of Pb (II) and Hg (II) from wastewater. A minimum dosage of 80 mg, 200 mg of BTMC is essential for the maximum removal of 95 % of Pb (II) and 93% of Hg (II) ion from synthetic wastewater.

Hence BTMC can be noted as an efficient adsorbent to remove nickel from wastewater due to its moderate ion-exchange property.

4. Conclusion

An economically efficient adsorbent for Pb (II) and Hg (II) removal was prepared from Mangosteen shell using sulphuric acid and sodium bicarbonate as modifiers. The manufacturing process is simple hence it can be used as an alternative for high-cost adsorbents. The mechanism of adsorption may be ion exchange process. The adsorption capacity (Q_0) of BTMC was found to be 58.98 mg g^{-1} and 49.75 mg g^{-1} for Pb (II) and Hg (II) respectively. The pseudo-second-order kinetics fits well showing that BTMC may follow the chemisorption process. Boyd's kinetic model predicts the actual rate-determining step involved in the adsorption process.

References

Abdulrasaq Osinfade O.O. and Basiru G. (2010), Removal of copper (II), iron (III) and lead (II) ions from Mono-component simulated waste effluent by adsorption on coconut husk, *African Journal of Environmental Science and Technology*, **4**(6), 82–387.

Ahmad R. and Haseeb S. (2012), Adsorption of Cu^{2+} from aqueous solution onto agricultural solid waste-menth: characterization, isotherms and kinetic studies, *Journal of Dispersion Science and Technology*, **33**, 1188–1196.

Akunwa N.K., Muhammad M.N. and Akunna J.C. (2014), Treatment of metal contaminated wastewater: a comparison of low-cost biosorbents, *Journal of Environmental Management*, **146**, 517–523.

Ayranci E. and Duman O. (2005), Adsorption behaviours of some phenolic compounds onto high specific area activated carbon cloth, *Journal of Hazardous Matter*, **124**, 125–132.

Bahrami A., Seidani A.B., Abbaspour A. and Shamsipur M. (2014), A highly selective voltammetric sensor for sub-nanomolar detection of lead ions using a carbon paste electrode impregnated with novel ion imprinted polymeric nano beads, *Electrochimica Acta*, **118**, 92–99.

Banerjee K., Ramesh S.T., Gandhimathi R., Nidheesh P.V. and Bharathi K.S. (2012), A novel agricultural waste adsorbent, watermelon shell for the removal of copper from aqueous solutions, *Iranica Journal of Energy and Environment*, **3** ,143–156.

Basu M., Guha A.K. and Ray L. (2017), Adsorption of lead on cucumber peel, *Journal of Cleaner Production*, **151,** 603-615.

Boyd G.E., Adamson A.W. and Myser L.S. (1947), The exchange adsorption of ions from aqueous solutions by organic zeolites, *Journal American Chemical Society*, **69**, 2836–2848.

Chen Y.D., Huang B., Huang M.J. and Cai B.Q. (2011), On the preparation and characterization of activated carbon from mangosteen shell, *Journal of Taiwan Institute of Chemical Engineers*, **42**, 83.

Coelho G.F., Gonçalves A.C., Tarley C.R.R., Casarin J., Nacke H. and Franciskowski M.A. (2014), Removal of metal ions Cd (II), Pb (II), and Cr (III) from water by the cashew nut shell Anacardium occidentale L, *Ecological Engineering*, **735**, 14–525.

Cruz C.C., Costa A.C., Henriques C.A. and Luna A.S. (2004), Kinetic modelling and equilibrium studies during cadmium biosorption by dead Sargassum Sp. Biomass, *Bioresource Technology*, **91**, 249–257.

Ebrahimzadeh H., Asgharinezhad A.A., Moazzen E., Amini M.M., Sadeghi O. (2015), A magnetic ion-imprinted polymer for lead

(II) determination: A study on the adsorption of lead (II) by beverages, *Journal of Food Composition and Analysis*, **41**, 74–80.

Ferreira B.C.S., Teodoro F.S., Mageste A.B., Gil L.F., de Freitas R.P. and Gurgel L.V.A. (2015), Application of a new carboxylate-functionalized sugarcane bagasse for adsorptive removal of crystal violet from aqueous solution: Kinetic, equilibrium and thermodynamic studies, *Industrial Crops and Products*, **65C**, 521–534.

Foo K.Y. and Hameed B.H. (2010), Insights into the modeling of adsorption isotherm systems, *Chemical Enineering Journal*, **156**, 2–10.

Gupta H. and Gogate P.R. (2016), Intensified removal of copper from wastewater using activated watermelon based biosorbent in the presence of ultrasound, *Ultrasonics Sonochemistry*, **30**, 113–122.

Hussein H., Farag S., Kandeel K. and Moawad H. (2004), Biosorption of heavy metals from wastewater using Pseudomonas sp. *Electronic Journal of Biotechnology*, **7(1)**, 38–46.

Ismaiel A.A., Aroua M.K. and Yusoff R. (2013), Palm shell activated carbon impregnated with task-specific ionic-liquids as a novel adsorbent for the removal of mercury from contaminated water, *Chemical Engineering Journal*, **225**, 306–314.

Jin G.P., Wang X.L., Fu Y. and Do Y. (2012), Preparation of tetraoxalyl ethylenediamine melamine resin grafted-carbon fibers for nano-nickel recovery from spent electroless nickel plating baths, *Chemical Engineering Journal*, **203,** 440–446.

Lakherwal D. (2014), Adsorption of heavy metals: A review. *International Journal of Environmental Research and Development*, **4**(1), 41–48.

Lam Y.F., Lee L.Y., Chua S.J., Lim, S.S. and Gan S. (2016), Insights into the equilibrium, kinetic and thermodynamics of nickel removal by environmental friendly Lansium domesticum peel biosorbent*, Ecotoxicology and Environmental Safety*, **127**, 61–70.

Lasheen M.R., Ammar N.S. and Ibrahim H.S. (2012), Adsorption/desorption of Cd (II), Cu (II) and Pb (II) using chemically modified orange peel: Equilibrium and kinetic studies*, Solid State Sciences*, **14**, 202–210.

Liu H., Zhang J., Ngo H.H., Guo W., Wu H., Cheng C., Guo Z. and Zhang, C. (2015), Carbohydrate-based activated carbon with high surface acidity and basicity for nickel removal from synthetic wastewater*, RSC Advances*, **5**, 52048–52056.

Mc Kay G., Blair S. and Garden J.R. (1982), Adsorption of dyes on chitin. I. Equilibrium studies, *Journal of Applied Polymer Science*, **27**, 3043.

Miretzky P., Munoz C. and Carrillo-Chavez A. (2008), Fluoride removal from aqueous solution by Ca-pretreated macrophyte biomass, *Environmental Chemistry,* **5**, 68–72.

Mostaedi M.T., Asadollahzadeh M., Hemmati A. and Khosravi A. (2013), Equilibrium, kinetic, and thermodynamic studies for biosorption of cadmium and nickel on grapefruit peel, *Journal of the Taiwan Institute of Chemical Engineers*, **44**, 295–302.

Ozer A. (2007), Removal of Pb (II) ions from aqueous solutions by sulphuric acid-treated wheat bran, *Journal of Hazardous Materials,* **141,** 753–761.

Pollard F.H., Hanson P. and Geary W.J. (1957), *Analytical chim Acta,* **20**, 26–31.

Rao M.M., Chandra Rao G.P., Seshaiah K., Choudary N.V. and Wang M.C. (2008), Activated carbon from Ceiba pentandra hulls, an agricultural waste, as an adsorbent in the removal of lead and zinc from aqueous solutions, *Waste Management*, **28**, 849–858.

Reddy D.H.K., Lae S. and Seshaiah K. ((2012)), Biosorption of toxic heavy metal ions from water environment using honeycomb biomass—an industrial waste material, *Water, Air, Soil Pollution,* **223**, 5967–5982.

Senthil Kumar P., Senthamarai C., Sai Deepthi A.S.L. and Bharani R. (2013), Adsorption isotherms, kinetics and mechanism of Pb(II) ions removal from aqueous solution using chemically modified agricultural waste, *The Canadian Journal of Chemical Engineering,* **91**, 1950–1956.

SenthilKumar P., Ramalingam S., DineshKirupha S,. Murugesan A., Vidhyadevi T. and Sivanesan S. (2011), Adsorption behavior of nickel (II) onto cashew nut shell: Equilibrium, thermodynamics, kinetics, mechanism and process design, *Chemical Engineering Journal*, **167**(1), 122–131.

Sharma A. and Bhattacharyya K.G. (2004), Adsorption of chromium (VI) on Azadirachta indica (Neem) leaf powder, *Adsorption*, **10**, 327–338.

Siddiqui S.H. and Ahmad R. (2017), Pistachio Shell Carbon (PSC) – an agricultural adsorbent for the removal of Pb (II) from aqueous solution, *Groundwater for Sustainable Development,* **4**, 42–48.

Sudha R., Srinivasan K. and Premkumar P. (2015), Removal of nickel (II) from aqueous solution using Citrus Limettioides peel and seed carbon, *Ecotoxicology and Environmental Safety*, **117**, 115–123.

Thuan T.V., Quynh B.T.P., Nguyen T.D., Ho V.T.T. and Giang L. (2017), Response surface methodology approach for optimization of Cu^{2+}, Ni^{2+} and Pb^{2+}adsorption using KOH-activated carbon from banana peel, *Surfaces and Interfaces*, **6**, 209–217.

Verma R. and Dwivedi P. (2013), Heavy metal water pollution-A case study, *Recent Research in Science and Technology*, **5(5),** 98–99.

Yao Z.Y., Qi J.H. and Wang L.H. (2010), Equilibrium, kinetic and thermodynamic studies on the biosorption of Cu (II) onto chestnut shell. *Journal of Hazardous Materials*, **174**, 137–143.

Zabihi M., Ahmadpour A. and Haghighi Asl A. (2009), Removal of mercury from water by carbonaceous sorbents derived from walnut shell, *Journal of Hazardous Materials*, **167**, 230–236.

Zadernowski R., Czaplicki S. and Naczk M. (2009), Phenolic acid profiles of mangosteen fruits (Garinia mangostana), *Food Chemistry*, **112**, 685.